PATTERNS & PHENOTYPES

N-RAP Expression During Mouse Heart Development

Shajia Lu,[1] **Diane E. Borst,**[2] **and Robert Horowits**[1]*

N-RAP gene expression and N-RAP localization were studied during mouse heart development using semiquantitative reverse transcriptase-polymerase chain reaction and immunofluorescence. N-RAP mRNA was detected at embryonic day (E) 10.5, significantly increased from E10.5 to E16.5, and remained essentially constant from E16.5 until 21 days after birth. In E9.5–10.5 heart tissue, N-RAP protein was primarily associated with developing premyofibril structures containing α-actinin, as well as with the Z-lines and M-lines of more-mature myofibrils. In contrast, N-cadherin was concentrated in patches at the periphery of the cardiomyocytes. N-RAP labeling markedly increased between E10.5 and E16.5; almost all of the up-regulated N-RAP was associated with intercalated disk structures, and the proportion of mature sarcomeres containing N-RAP decreased. In adult hearts, specific N-RAP staining was only observed at the intercalated disks and was not found in the sarcomeres. The results are consistent with N-RAP functioning as a catalytic scaffolding molecule, with low levels of the scaffold being sufficient to repetitively catalyze key steps in myofibril assembly. *Developmental Dynamics 233:201–212, 2005.* Published 2005 Wiley-Liss, Inc.†

INTRODUCTION

N-RAP is an actin-binding LIM protein that is concentrated at the ends of striated muscle cells (Luo et al., 1997; Zhang et al., 2001; Mohiddin et al., 2003). The N-RAP gene structure and coding sequence are highly conserved between mice and humans. As illustrated in Figure 2A, in both species, the protein consists of an N-terminal LIM domain followed by repetitive actin-binding modules that are homologous to those found in nebulin (Mohiddin et al., 2003), a giant protein that is thought to act as a length-regulating template for sarcomeric actin filaments in skeletal muscle (Kruger et al., 1991; Labeit et al., 1991; Labeit and Kolmerer, 1995; Wang et al., 1996). The N-RAP repeats are arranged as a series of five C-terminal super repeats, each composed of seven single repeats. In between the LIM domain and super repeats are 10 or 11 single repeats. Alternative splicing of N-RAP has been reported for exon 12 (Mohiddin et al., 2003; Gehmlich et al., 2004) and exon 39 (Gehmlich et al., 2004). Each of these exons encodes a single 35- to 36-residue module. In both humans and mice, exon 12 is not expressed in adult cardiac muscle but is included in ~90% of the N-RAP transcripts in adult skeletal muscle;

therefore, the full-length N-RAP isoforms that include or exclude exon 12 have been termed N-RAP-s and N-RAP-c, for skeletal and cardiac muscle, respectively (Mohiddin et al., 2003).

At the ultrastructural level, N-RAP is localized to the terminal actin bundles that link myofibrils to membrane complexes at the myotendinous junctions in skeletal muscle and at the intercalated disks in heart muscle (Herrera et al., 2000; Zhang et al., 2001). In hearts, these terminal actin bundles are found in the adherens junction region of the intercalated disk (Forbes and Sperelakis, 1985;

Severs, 1995), providing for transmission of myofibrillar force to the membrane and to neighboring cells by means of cadherin linkages between cardiomyocytes (Takeichi, 1990; Geiger and Ayalon, 1992; Kemler, 1993; Hertig et al., 1996). The predominant form of cadherin in heart tissue is N-cadherin, which appears in the precardiac mesoderm at E7.5 in the mouse embryo (Radice et al., 1997).

N-RAP, N-cadherin, and connexin-43 copurify with cardiac intercalated disks. N-RAP also remains tightly bound at the ends of isolated myofibrils (Zhang et al., 2001). These tight associations suggest a mechanical linking function for N-RAP; consistent with this suggestion, N-RAP–binding partners include several cytoskeletal proteins that are concentrated at intercalated disks or myotendinous junctions. These proteins include talin, vinculin and actin (Luo et al., 1999), filamin (Lu et al., 2003), MLP (muscle LIM protein; Ehler et al., 2001; Gehmlich et al., 2004), and α-actinin (Zhang et al., 2001; Lu et al., 2003).

Although subcellular localization and biochemical copurification from adult muscles suggested that N-RAP may link the ends of myofibrils to membrane-associated protein complexes, studies in cultured embryonic cardiomyocytes have implicated N-RAP in myofibril assembly (Carroll and Horowits, 2000; Carroll et al., 2001, 2004; Lu et al., 2003). These studies showed that N-RAP localizes with the earliest myofibril precursors that originate near the membrane (Carroll and Horowits, 2000; Lu et al., 2003). These precursors contain punctate α-actinin Z-bodies, α-actin, and muscle tropomyosin (Dlugosz et al., 1984; Wang et al., 1988; Schultheiss et al., 1990; Handel et al., 1991; Rhee et al., 1994; Dabiri et al., 1997), as well as nonmuscle myosin IIb (Rhee et al., 1994). Time-lapse studies of living cardiomyocytes expressing green fluorescent protein (GFP) -tagged α-actinin showed that the Z-bodies aggregate laterally to form nascent myofibrils (Dabiri et al., 1997). Muscle myosin gradually replaces the nonmuscle isoform (Dabiri et al., 1997), and titin is incorporated as well. Other studies suggest that bipolar muscle myosin filaments may form

separately from the I-Z-I structures and that the integration of these myosin filaments may be controlled by interactions with titin (Schultheiss et al., 1990; Holtzer et al., 1997). When the N-RAP LIM domain, single-repeat region, or super repeats were individually expressed as GFP fusion proteins in cardiomyocytes, myofibril assembly was disrupted (Carroll et al., 2001, 2004). In contrast, expression of a truncated N-RAP construct, which contained the LIM domain and single repeats but omitted the super repeats, permitted assembly of α-actinin into mature Z-disks but disrupted sarcomeric actin organization (Carroll et al., 2004). These results are consistent with a scaffolding model for myofibrillogenesis in which N-RAP controls the assembly of α-actinin and actin into symmetrical I-Z-I structures, with the barbed end of actin filaments anchored to α-actinin at the Z-line and the pointed ends of the actin filaments extending in either direction toward the middle of the sarcomere (Carroll et al., 2004).

In the present work, we study N-RAP accumulation and localization in the embryonic mouse heart relative to developing myofibrils and intercalated disks. We find a transient association of low levels of N-RAP with myofibril precursors and newly formed sarcomeres, with larger amounts of N-RAP associated with developing intercalated disks. The results are consistent with N-RAP functioning as a catalytic scaffolding molecule, with low levels of the scaffold being sufficient to repetitively catalyze key steps in sarcomere assembly.

RESULTS

Specificity of N-RAP Expression

Figure 1 shows immunofluorescence detection of N-RAP and sarcomeric α-actinin in frozen sections of E10.5 and E13.5 mouse embryos. At E10.5, the heart is clearly seen as the only area positive for sarcomeric α-actinin, and the N-RAP protein is detected as a low level of specific staining that is not present in neighboring nonmuscle tissue. By E13.5, the heart is well-developed, and other major internal

organs are clearly visible. N-RAP expression is confined to the heart and developing skeletal muscles, which are specifically labeled with the sarcomeric α-actinin antibody.

N-RAP, α-Actinin, and N-Cadherin Transcript Accumulation During Cardiac Development

We used reverse transcriptase-polymerase chain reaction (RT-PCR) to amplify specific regions of the N-RAP transcript and to monitor N-RAP mRNA accumulation during cardiac development. Specific primers were chosen to amplify N-RAP exons 9–14 and exons 36–41 (Fig. 2A–C). We previously showed that N-RAP exon 12 is not expressed in adult hearts (Mohiddin et al., 2003). By using the exon 9–14 primers, we observed a single PCR product from cardiac tissue between E10.5 and P21 that is consistent with omission of exon 12; the cardiac transcript in this region is 105 bases smaller than the predominant product from adult skeletal muscle, which includes exon 12 (Fig. 2B). Amplification of N-RAP exons 36–41 yielded a single product at the predicted size, with no evidence for alternate splicing in this region at any stage of cardiac development (Fig. 2C). N-RAP expression significantly increased between E10.5 and E16.5 and remained relatively constant between E16.5 and P21. At E10.5, N-RAP expression was ~3% of its maximum level (Fig. 2B,C).

We also investigated α-actinin and N-cadherin transcript accumulation during heart development. Single clear bands were amplified from cardiac tissue using the α-actinin primers (Fig. 2D), which were designed to amplify transcripts from the two muscle forms of α-actinin, α-actinin-2, and α-actinin-3 (Mills et al., 2001). The N-cadherin primers also amplified a single band at all stages of heart development (Fig. 2E). In contrast to N-RAP, α-actinin and N-cadherin transcripts were each greater than half-maximal by E10.5 and reached maximum levels by E13.5 (Fig. 2D,E).
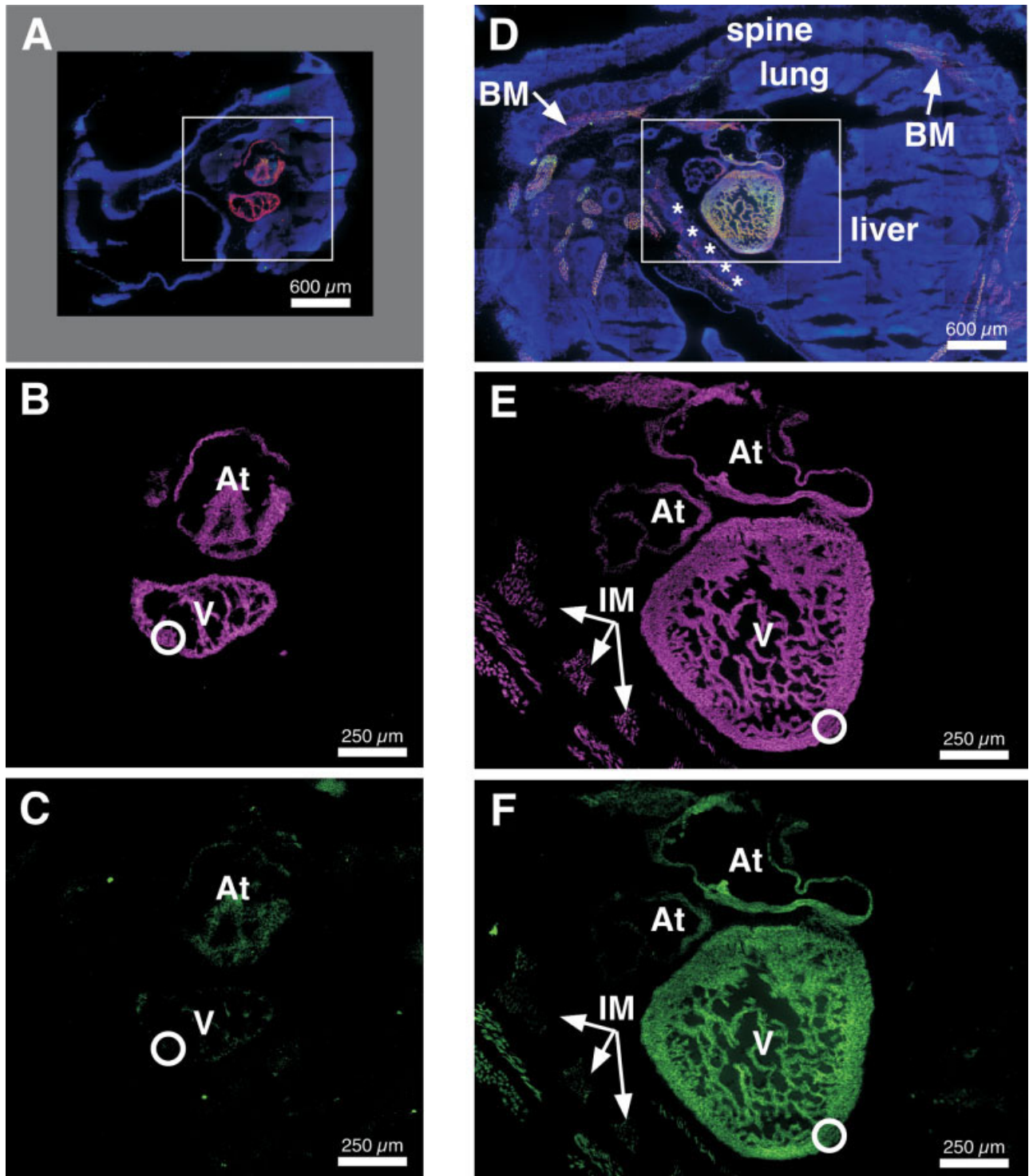
Fig. 1. A–F: Immunofluorescence detection of N-RAP and α-actinin in sections of embryonic day (E) 10.5 (A–C) and E13.5 (D–F) embryos. **A,D:** Shown are N-RAP, α-actinin, and 4′,6-diamidino-2-phenylindole-dihydrochloride (DAPI) staining as green, red, and blue channels, respectively. **B,C,E,F:** The boxed areas in A and D are enlarged in the lower panels, which show α-actinin staining as magenta (B,E) and N-RAP staining as green (C,F). A–C: At E10.5, the cardiac atrium (At) and ventricle (V) stains heavily for α-actinin, and lightly for N-RAP. D–F: At E13.5, N-RAP and α-actinin staining is observed in the cardiac atria (At) and ventricle (V), as well as in developing skeletal muscles, whereas nonmuscle tissues such as the lung, liver, spine, and ribs (asterisks) do not accumulate N-RAP or α-actinin. Back muscles (BM) and intercostal muscles (IM) are labeled. The circled regions in B,C and E,F indicate the areas shown at high magnification in Figures 3 and 4, respectively. Images are collages assembled from overlapping photomicrographs taken with a ×10 objective.
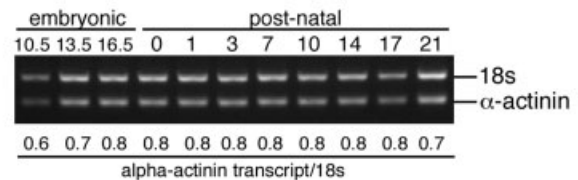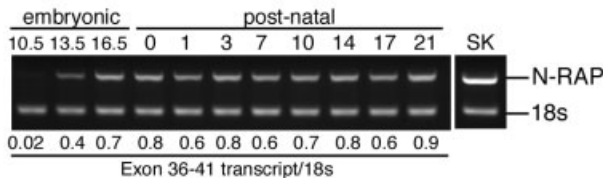
A. N-RAP Exons & Domains
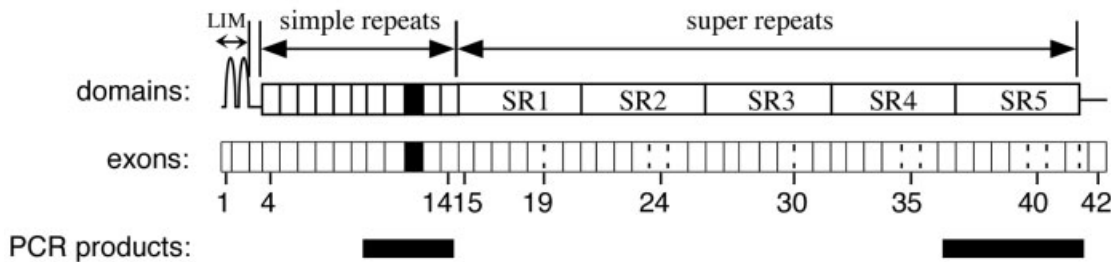
B. N-RAP exons 9-14
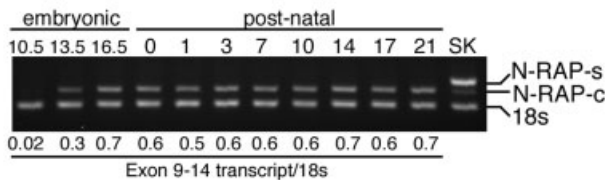
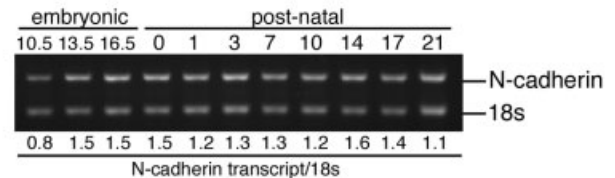## C. N-RAP exons 36-41

D. α-actinin

E. N-cadherin

Fig. 2. A: N-RAP domain organization and corresponding exons (Mohiddin et al., 2003). Exons 1 and 2 together encode a LIM domain; exons 4–14 encode single repeating modules; and exons 15–41 encode five super repeats, each of which contains seven single modules. Exon boundaries correspond to module boundaries, except where dashed vertical lines indicate multiple modules encoded by a single exon. Exon 12 is alternatively spliced (filled box). The location of polymerase chain reaction (PCR) products is illustrated below the domain and exon maps. **B–E:** PCR products amplified from cDNA made from RNA isolated from mouse heart tissue. Numbers above the gels refer to embryonic or postnatal days of development, as indicated, where postnatal day 0 is the day of birth. N-RAP was also amplified from mouse skeletal muscle cDNA for comparison (SK). N-RAP-s and N-RAP-c refer to isoforms containing or omitting N-RAP exon 12. Adult mouse skeletal muscle expresses both N-RAP isoforms (B, lane SK). 18s rRNA was amplified as an internal control. Numbers below the gels are the relative levels of specific transcripts normalized to the internal 18s controls; this method is valid for assessing changes in the levels of each particular mRNA species during development but is not suitable for comparing the relative amounts of mRNA derived from different genes. (See text for details.)

N-RAP Association With Developing Myofibrils

We used antibody staining of sarcomeric α-actinin as a marker for developing and mature myofibrils. In the E10.5 heart, closely spaced dots or narrow bands of α-actinin typical of myofibril precursors were seen. More-mature myofibrils characterized by periodic, broad bands of α-actinin were also present (Fig. 3). In double-stained sections, N-RAP is associated with the myofibril precursors, as well as with more-mature myofibrils. In the latter case, N-RAP is organized into striations with twice the α-actinin periodicity, colocalizing with α-actinin at the Z-line and producing an additional band of staining at the center of the sarcomere (Fig. 3).

At E13.5, bright patches of N-RAP staining were observed, some of which colocalized with α-actinin (Fig. 4, arrows). Myofibril precursors, characterized by punctate α-actinin organization, were also seen, and N-RAP was associated with these structures as well (Fig. 4, asterisks). N-RAP staining associated with more-mature myofibrils in E13.5 hearts was faint and variable. In some sarcomeres, N-RAP staining was seen at both the Z-line and at the center of the sarcomere (Fig. 4, arrowheads 1), whereas in other regions, N-RAP staining was mainly confined to the center of the sarcomere (Fig. 4, arrowheads 2). Sarcomeres with very broad-banded α-actinin striations are presumably the most-mature structures, and N-RAP staining was barely detectable in these regions (Fig. 4, arrowheads 3).

In newborn animals, N-RAP staining was predominantly found in bright patches, often as closely spaced doublets (Fig. 5, arrows). Very faint staining in sarcomeres could sometimes also be observed. In adult hearts, N-RAP staining was concentrated at the ends of the cardiomyocytes, at the intercalated disks (Fig. 6, arrows). No specific N-RAP staining was observed in mature myofibrils in adult hearts.
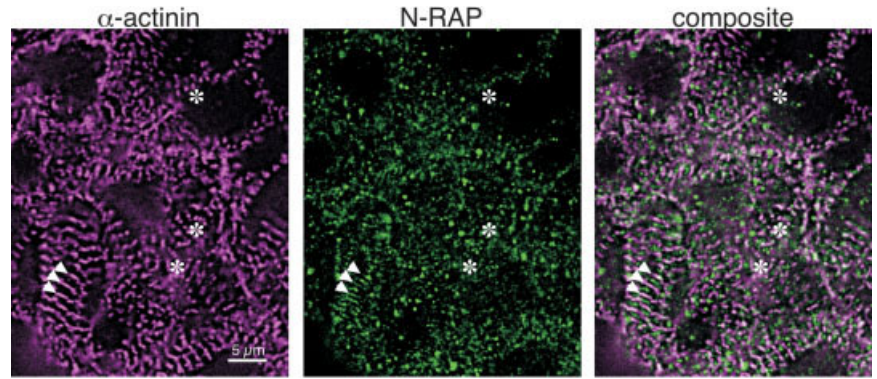
Fig. 3. Localization of α-actinin (magenta) and N-RAP (green, top row) or α-actinin (magenta) and the nonimmune control (green, bottom row) in a mouse embryonic day 10.5 heart. Myofibrils marked by periodic bands of α-actinin (arrowheads), as well as closely spaced dots or narrow bands of α-actinin typical of myofibril precursors (asterisks), are present. N-RAP is associated with the myofibril precursors and stains at twice the α-actinin periodicity in more-mature myofibrils (arrowheads). Symbols are used to mark identical regions in the corresponding magenta, green, and composite images. Nonspecific punctate staining is evident with the nonimmune serum at this stage, put the nonspecific staining is not correlated with α-actinin staining.
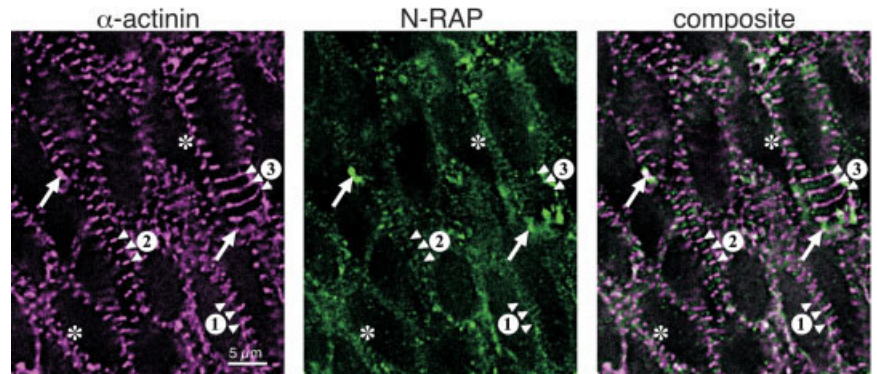

Fig. 4. Localization of α-actinin (magenta) and N-RAP (green, top row) or α-actinin (magenta) and the nonimmune control (green, bottom row) in a mouse embryonic day (E) 13.5 heart. Myofibrils marked by periodic bands of α-actinin (arrowheads), as well as closely spaced dots or narrow bands of α-actinin typical of myofibril precursors (asterisks), are present. Faint but specific N-RAP staining is associated with the myofibril precursors. In more-mature myofibrils, N-RAP staining may be present at both the Z-line and at the center of the sarcomere (arrowheads 1), confined to the center of the sarcomere (arrowheads 2), or barely detectable (arrowheads 3). Bright patches of N-RAP staining are also present (arrows). Symbols are used to mark identical regions in the corresponding magenta, green, and composite images.
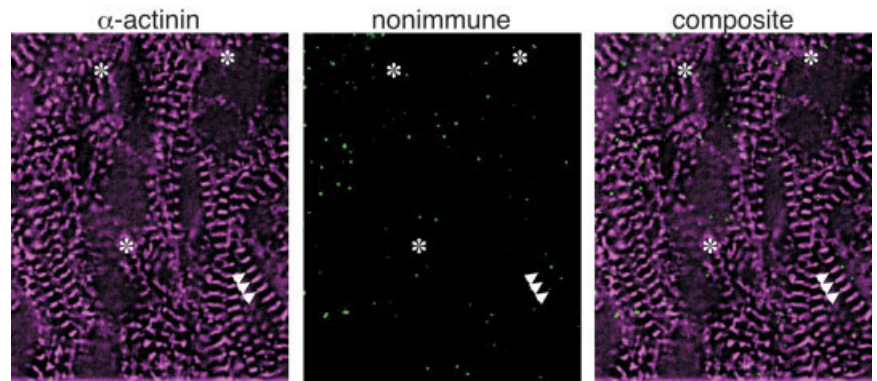
Fig. 5. Localization of α-actinin (magenta) and N-RAP (green, top row) or α-actinin (magenta) and the nonimmune control (green, bottom row) in a mouse newborn heart. Most of the N-RAP staining is in bright patches, often as closely spaced doublets containing α-actinin (arrows). Faint staining in sarcomeres can sometimes be observed.
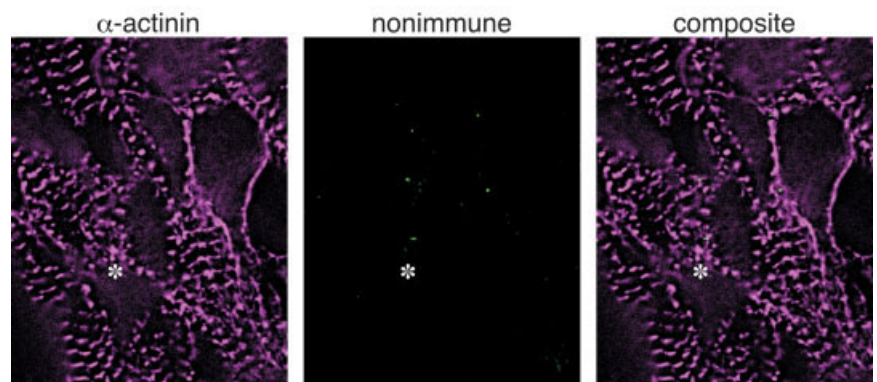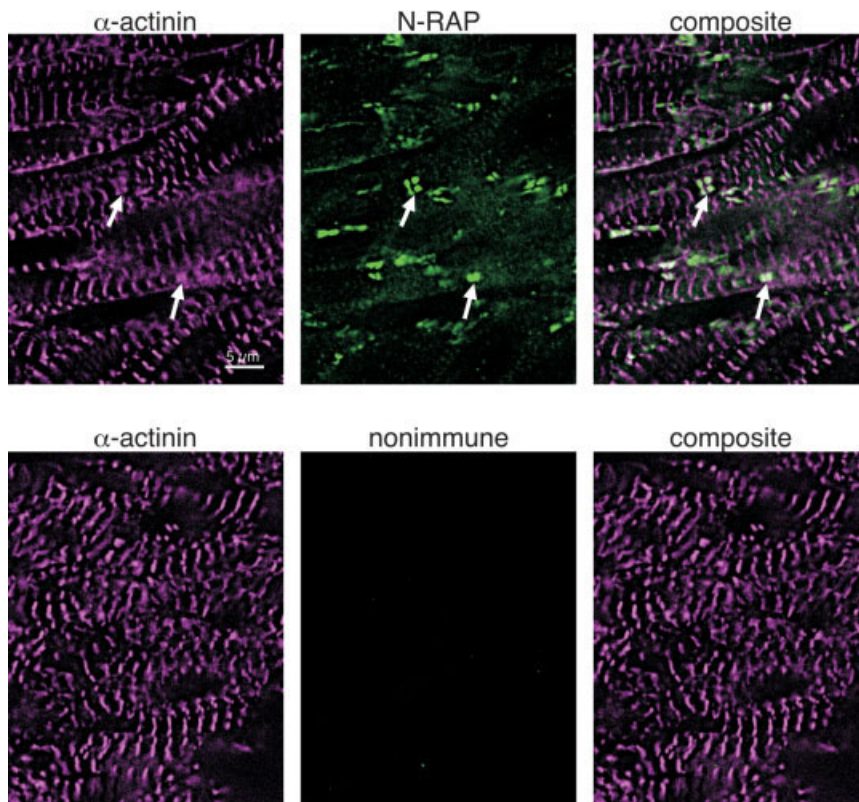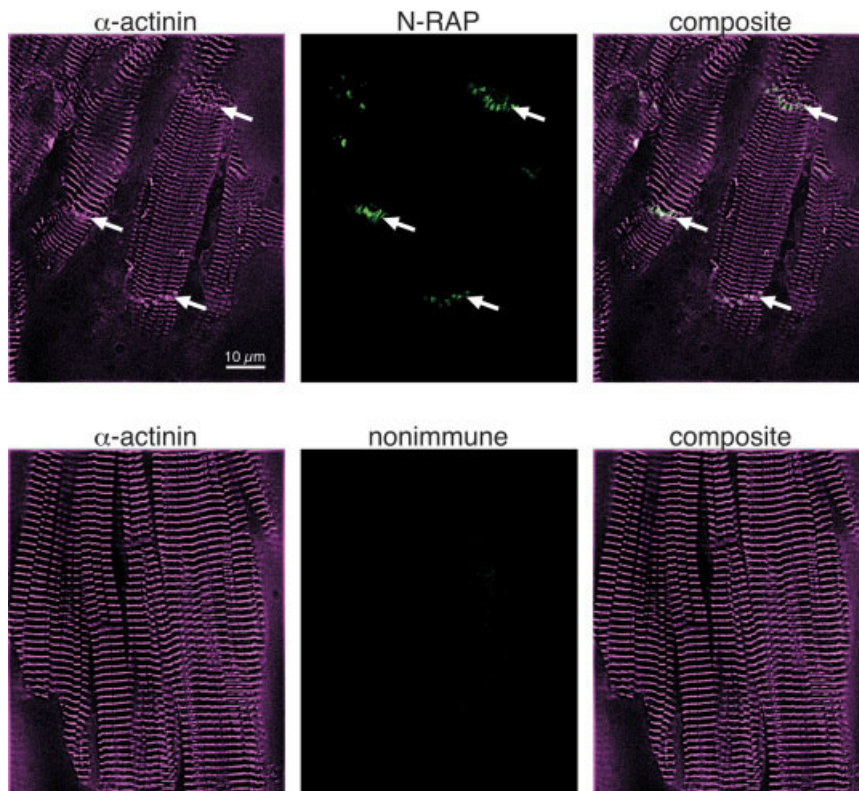
Fig. 6. Localization of α-actinin (magenta) and N-RAP (green, top row) or α-actinin (magenta) and the nonimmune control (green, bottom row) in a mouse adult heart. N-RAP staining is concentrated at the ends of the cardiomyocytes, at the intercalated disks (arrows). No specific N-RAP staining is observed within the mature myofibrils.
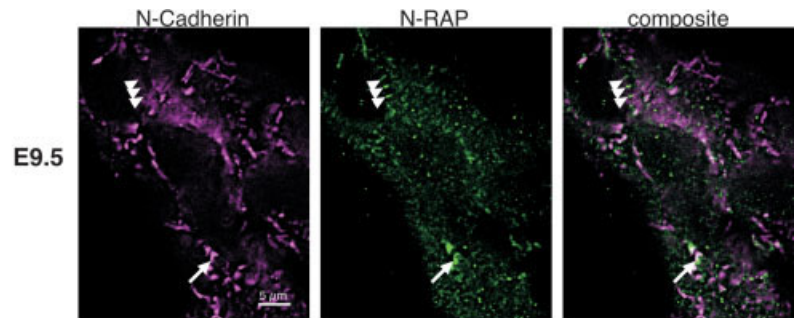
Fig. 7. Localization of N-cadherin (magenta) and N-RAP (green) in a mouse embryonic day (E) 9.5 heart tube (top row) and E13.5 heart (bottom row). N-cadherin is distributed in bright patches at the periphery of the cells (arrows). At E9.5, N-RAP is only occasionally concentrated in these patches, but by E13.5, much of the N-RAP labeling is organized as doublets bracketing a central patch of N-cadherin. Periodic N-RAP staining characteristic of sarcomeric organization is also seen at E9.5, but these structures do not contain N-cadherin (arrowheads).
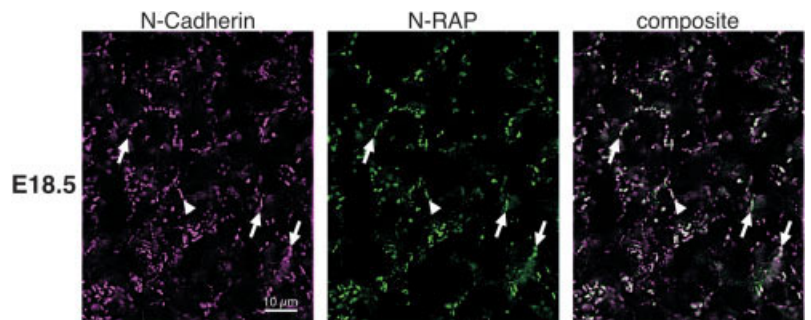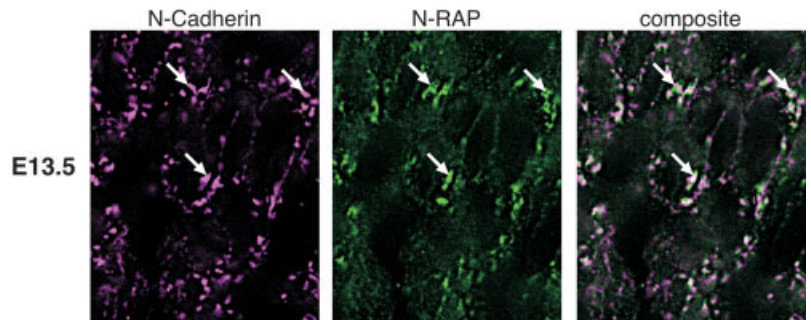
Fig. 8. Localization of N-cadherin (magenta) and N-RAP (green) in a mouse embryonic day (E) 18.5 heart (top row) and adult heart (bottom row). By E18.5, most of the N-RAP and N-cadherin is colocalized in bright patches, often as linear structures (arrows). Closely spaced doublets of N-RAP staining surrounding a central band of N-cadherin staining are occasionally observed (arrowhead). In adult hearts, both N-RAP and N-cadherin are concentrated at the ends of the cardiomyocytes, at the intercalated disks.
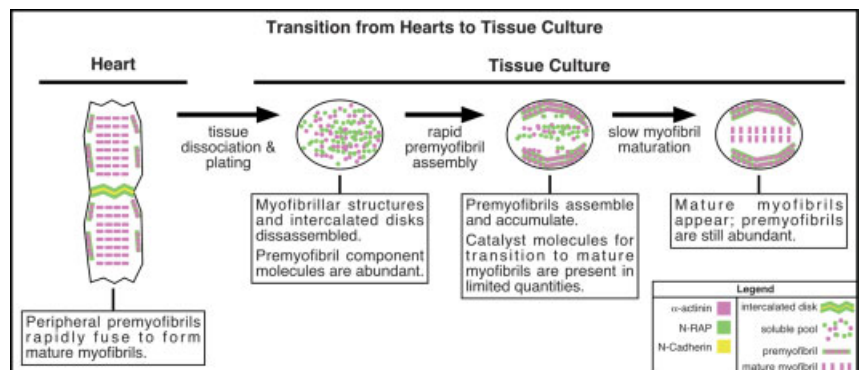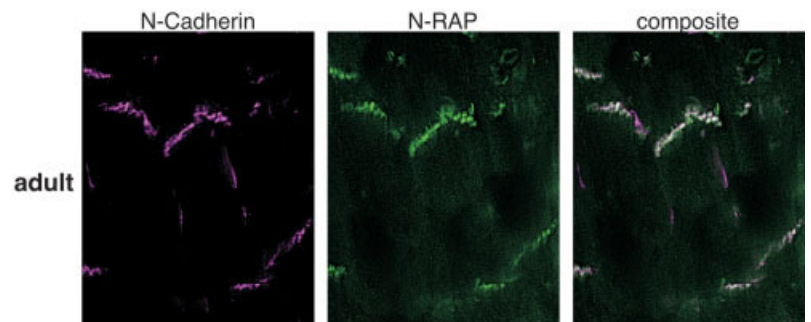
Fig. 9. Distribution of myofibrillar components in embryonic hearts and reorganization upon dissociation and plating of cells.

N-RAP Association With Developing Intercalated Disks

In the E9.5 heart tube, N-cadherin was concentrated in bright patches along the periphery of cells. At this stage, N-RAP staining was only rarely colocalized with N-cadherin (Fig. 7). Most of the N-RAP staining was faint and diffuse or organized as closely spaced dots or narrow striations that are not associated with N-cadherin (Fig. 7, top row). By E13.5, much of the N-RAP staining was organized in bright patches that colocalize or bracket N-cadherin, but very faint periodic N-RAP staining is also present in some areas (Fig. 7, bottom row).

In E18.5 hearts, most of the N-RAP staining was in bright patches, sometimes as closely spaced doublets surrounding a central band of N-cadherin staining (Fig. 8, top row). At this time, the N-cadherin/N-RAP–positive patches also appear to have started aligning to form larger linear structures. In adult hearts, these have developed into the mature intercalated disks, which are clearly apparent at the ends of longitudinally oriented myocytes (Fig. 8, bottom row). In adult hearts, N-RAP is concentrated at the intercalated disks, and no specific N-RAP staining was observed in the myofibrils.

DISCUSSION

N-RAP Alternative Splicing

Previously, we showed that N-RAP exon 12 is alternately spliced, being expressed in adult skeletal muscle but not in adult cardiac muscle (Mohiddin et al., 2003). The current results show that, throughout mouse heart development, only the cardiac isoform of N-RAP is expressed; at no stage of murine development was N-RAP exon 12 detected in the heart. Recently, Furst and colleagues reported alternate splicing of N-RAP exon 39 in humans, but these authors did not report on the tissue specificity of this splicing event (Gehmlich et al., 2004). In the mouse, we found no evidence for alternative splicing in N-RAP exons 36–41 throughout cardiac development or in adult skeletal muscle.

N-RAP Association With Developing Myofibrils and Intercalated Disks

The semiquantitative RT-PCR method used for assessing transcript accumulation relied on using the 18s rRNA as an internal control for normalization in a duplex PCR reaction. Because rRNA is so much more abundant than any mRNA, the efficiency of amplifying the 18s RNA product was reduced by using nonpriming competimers mixed with the 18s RNA primers; the appropriate competimer to primer ratio was empirically determined to bring the 18s product into the linear range of detection with the same number of amplification cycles needed for measuring mRNA levels. This method is suitable for assessing changes in the levels of a particular mRNA species during development but cannot be used to determine the relative amounts of mRNA derived from different genes.

Overall, the time-course of N-RAP mRNA accumulation lagged that of the N-cadherin and α-actinin mRNAs. We detected low levels of N-RAP expression as early as E10.5, with N-RAP expression increasing to a maximum, constant level by E16.5. In contrast, both N-cadherin and α-actinin were expressed at half-maximum levels by E10.5, and each reached a constant maximum level by E13.5.

Our results are consistent with previous work showing that N-cadherin is highly expressed in the precardiac mesoderm of developing mouse embryos (Radice et al., 1997). Genetic deletion of N-cadherin disrupts heart formation. However, cultured myocytes derived from N-cadherin knockout mice can form loose aggregates and beat in culture, showing that N-cadherin is not essential for cardiac myocyte differentiation (Radice et al., 1997). Although not essential for myofibril assembly, inhibition of N-cadherin function through specific antibodies does inhibit myofibril assembly in cultured cardiomyocytes (Soler and Knudsen, 1994) or precardiac explants (Imanaka-Yoshida et al., 1998).

Our data shows that, in the early stages of heart development, N-RAP is associated with developing myofibrils marked by α-actinin staining as well as with developing intercalated disks marked by N-cadherin staining. As N-

RAP is up-regulated during cardiogenesis, most of the N-RAP is colocalized with N-cadherin in developing intercalated disks, whereas only a small part of the total N-RAP is associated with developing myofibrils. Nevertheless, the early association of N-RAP with myofibril precursors and its transient association with the Z-lines of newly formed myofibrils is consistent with the model of N-RAP as an organizing center for α-actinin and actin assembly in the first steps of myofibrillogenesis (Carroll et al., 2001, 2004). The low levels of N-RAP involved are consistent with N-RAP functioning as a catalytic scaffolding molecule, with low levels of the scaffold being sufficient to repetitively catalyze assembly. However, transient localization of N-RAP at the center of newly formed sarcomeres was unexpected and remains to be explained.

Embryonic Hearts Versus Cultured Cardiomyocytes

Recently, a debate has emerged regarding the general relevance of features of myofibril assembly observed in spreading cultured cardiomyocytes when compared with myofibril assembly in systems that retain three-dimensional cellular organization as seen in living embryos. Investigators studying myofibril assembly in cultured cardiomyocytes (Rhee et al., 1994; Dabiri et al., 1997), precardiac mesoderm explant cultures (Imanaka-Yoshida et al., 1998; Rudy et al., 2001), and embryonic hearts (Ehler et al., 1999) agree that the earliest myofibril precursors originate near the membrane but disagree about other details. In particular, large areas containing nonmuscle myosin IIb and periodic α-actinin dots with submicron spacing are found at the periphery of spreading cultured avian cardiomyocytes (Rhee et al., 1994; Carroll and Horowits, 2000; Lu et al., 2003) as well as in explant cultures (Imanaka-Yoshida et al., 1998; Du et al., 2003) but are not as prominent in embryonic avian hearts (Ehler et al., 1999). We found that closely spaced α-actinin dots consistent with premyofibril formation are present in embryonic mouse hearts but are less evident than in the spreading cultured cardiomyocytes. Likewise, we found ex-

tremely low levels of N-RAP staining associated with myofibril precursors in embryonic hearts (this report), whereas higher levels of N-RAP staining were associated with the large areas of peripheral premyofibrils seen in cultured cells (Carroll and Horowits, 2000; Lu et al., 2003).

These results are most easily understood by considering the effects of dissociation and plating of cardiomyocytes on the pool of molecules participating in myofibril assembly, as shown schematically in Figure 9. In the embryo, α-actinin staining is largely confined to myofibrillar structures, with no evidence for a large unassembled pool. Likewise, closely spaced α-actinin dots characteristic of premyofibrils are present, but are rare, suggesting that intermediate states of assembly are relatively short-lived (Figs. 3, 4). Dissociation and plating of beating cardiomyocytes results in rounding up of the cells and disassembly of the preexisting myofibrils, followed by spreading and reassembly (Lin et al., 1989; Rhee et al., 1994; Carroll and Horowits, 2000; Carroll et al., 2001; Fig. 9). The large pool of cytoplasmic proteins involved in assembly can, in principal, drive accumulation of premyofibril structures. This pool can include both structural components that come from disassembly of the existing myofibrils as well as scaffolding molecules that are present in substoichiometric amounts but function as catalysts for particular steps in assembly. After plating and disassembly of existing myofibrils, the unassembled structural components are abundant, and the assembly rate may be limited by restricted availability of the catalytic scaffolds. Premyofibrils assemble in quantity, indicating that the structural components and catalytic scaffolding molecules required for the first steps in assembly are present in sufficient quantities. The large pool of N-RAP sequestered at developing intercalated disks in the embryo is probably released during cell dissociation and plating, becoming available to function in myofibril assembly. The accumulation of assembly intermediates such as premyofibrils in the cultured cells indicates that subsequent steps in assembly become rate limiting, suggesting limited availability of

downstream structural components or catalysts. One possible candidate for a downstream assembly catalyst is Krp1, which organizes between laterally fusing myofibril precursors in the final steps of assembly (Lu et al., 2003). The model in Figure 9 reconciles the quantitative differences observed between embryos and cultured cells, without the need to invoke qualitative differences in the mechanism of myofibril assembly.

The precardiac mesoderm explant culture system exhibits some quantitative features of myofibril assembly that are similar to developing embryos, while also exhibiting features of assembly characteristic of spreading cardiomyocyte cultures (Imanaka-Yoshida et al., 1998; Rudy et al., 2001; Du et al., 2003). Myofibril assembly in the explant cultures occurs de novo from newly synthesized proteins, as observed in embryos. Accordingly, the sarcomeric forms of α-actinin and myosin are not expressed shortly after explant, but accumulate after 10 hr (Imanaka-Yoshida et al., 1998; Du et al., 2003). Nevertheless, a diffusely staining pool of sarcomeric α-actinin appears to accumulate in early stages of myofibril assembly in this system (Imanaka-Yoshida et al., 1998), reminiscent of spreading cardiomyocyte cultures shortly after plating (Carroll and Horowits, 2000). In intermediate stages of assembly, periodic α-actinin dots with submicron spacing are more evident at the periphery of the cardiomyocytes in explant cultures (Imanaka-Yoshida et al., 1998; Du et al., 2003) than in embryos (Ehler et al., 1999, and this report). The evidence suggests that myofibril assembly is most efficient in the embryo, where assembly proceeds to completion and assembly intermediates do not accumulate; that assembly is less efficient in the explant cultures, where modest accumulations of assembly intermediates are observed; and that assembly is least efficient in the dissociated, spreading cardiomyocyte cultures.

CONCLUSIONS

In summary, the early association of N-RAP with developing myofibrils is consistent with N-RAP functioning as a catalytic scaffolding molecule in the

earliest stages of myofibril assembly. The function of the relatively large amounts of N-RAP that subsequently accumulate at the intercalated disks is unknown. One possibility is that these may serve as a reserve of molecules poised to quickly initiate assembly at the ends of the cell. Another possibility is suggested by N-RAP's apparent involvement in pathways leading to cardiomyopathy. N-RAP is up-regulated early in two genetic mouse models of dilated cardiomyopathy (Ehler et al., 2001). Both mouse models lead to decreased cardiac expression of MLP, one by genetic ablation (Arber et al., 1997), the other as a secondary effect of transgenic overexpression of tropomodulin (Sussman et al., 1998; Ehler et al., 2001). MLP is found at myofibrillar Z-lines and vinculin-positive junctional sites (Arber et al., 1997), as well as in the nucleus of differentiating myotubes, where it may regulate gene expression through interaction with transcription factors (Arber et al., 1994; Kong et al., 1997). MLP mutations have recently been linked to cases of hypertrophic cardiomyopathy and dilated cardiomyopathy in humans (Knoll et al., 2002; Geier et al., 2003). One of these mutations disrupts MLP binding to both N-RAP and α-actinin in vitro (Gehmlich et al., 2004), suggesting that interaction of MLP with N-RAP and α-actinin may influence cardiac architecture. Therefore, a structural or signaling function for N-RAP at the cardiac intercalated disks is an attractive hypothesis for future studies.

EXPERIMENTAL PROCEDURES

Animals

Timed pregnant CD-1 mice were purchased from Charles River Laboratories (Wilmington, MA). All animal handling procedures were performed under a National Institutes of Health animal study proposal approved by the NIAMS Animal Care and Use Committee.

RNA Purification

Freshly dissected tissue was placed in RNAlater RNA stabilization solution (Ambion, Inc., Austin, TX) and stored

TABLE 1. PCR Primer Pairs

Amplified mRNA	Primer pair
N-RAP, exons 9–14	Forward: 5′–GACCGATGTGGCCAGGTTTACTCAGAAG–3′
	Reverse: 5′–CAGGGGAACCAGCCTCATCGTTGTTTG–3′
N-RAP, exons 36–41	Forward: 5′–TGATGGGCATGAAAGGGACAGGAT–3′
	Reverse: 5′–ATCCCCGGGCCCCTCCTGTT–3′
α-actinin	Forward: 5′–ATCATCCTCCGCTTCGCCATTC–3′
	Reverse: 5′–TCTTCAGCATCCAACATCTTAGG–3′
N-Cadherin	Forward: 5′–TTCCACCTCGCTGTAAAAATGG–3′
	Reverse: 5′–TTATTCAGAACGCTGGGGTCAG–3′

at −70°C until used. Tissue was homogenized in TRIzol reagent (Invitrogen Corporation, Carlsbad, CA) using a FastPrep Instrument with lysing Matrix D set for 20 sec at speed 5 (Qbiogene, Inc., Carlsbad, CA). Total RNA was isolated using TRIzol reagent (Invitrogen Corporation) according to the manufacturer's protocol, based on the method of Chomczynski and Sacchi (Chomczynski and Sacchi, 1987). Contaminating DNA was removed using the DNA-free Kit (Ambion Inc.), and the purified RNA samples were stored at −80°C.

Semiquantitative RT-PCR

cDNA was synthesized from 0.5 μg of total RNA using the Advantage RT-for-PCR Kit (BD Biosciences Clontech, Palo Alto, CA) with random hexamers as primers. Defined regions of the mouse N-RAP, α-actinin, and N-cadherin transcripts were amplified using the primer pairs detailed in Table 1. The amplification protocol used for N-RAP and N-cadherin was 1 cycle at 95°C for 1 min; 30 cycles at 95°C for 30 sec, then 68°C for 1 min; and then 1 cycle at 68°C for 1 min. The amplification protocol used for α-actinin was 1 cycle at 95°C for 1 min; 30 cycles at 95°C for 30 sec, then 64°C for 1 min; and then 1 cycle at 68°C for 1 min.

To evaluate mRNA levels quantitatively, pilot experiments were conducted in which the number of PCR cycles was varied to determine the linear range of PCR product detection. Duplex RT-PCR reactions were run using ribosomal 18s RNA as an internal standard. Ambion's competimer technology was used to bring the control RNA into the linear range of detection using the same cycle numbers as needed for the experimental tran-

script. QuantumRNA 18s (universal 315 bp, or classic 488 bp) Internal Standard primers (Ambion, Inc.) were used to modulate amplification efficiency of the 18s RNA without affecting amplification of the target genes in a duplex PCR reaction. The appropriate ratio of 18s rRNA primers to competimers (blocked primers, which bind the target but cannot be elongated) was determined experimentally for each target gene and PCR condition.

All PCR experiments were performed using a PTC-200 Peltier Thermal Cycler (MJ Research, Inc., Waltham, MA). Amplicons were visualized on 1.5% agarose gels containing ethidium bromide. Gel images were captured by using a Kodak Image Station 440CF (Eastman Kodak Company, New Haven, CT). Quantitative image analysis was performed on a Macintosh computer using the public domain NIH Image program (developed at the US National Institutes of Health and available on the Internet at http://rsb.info.nih.gov/nih-image/). The level of target gene expression was normalized against the 18s rRNA control in the same PCR reaction.

Antibodies

Rabbit polyclonal antibody against N-RAP has been described previously and was used at a dilution of 1:1,000 (Luo et al., 1997). Monoclonal antibody against sarcomeric α-actinin (clone EA-53) was used at a dilution of 1:2,000 (Sigma-Aldrich, St. Louis, MO). Monoclonal antibody against N-cadherin (RDI-NCADHERabm) was used at a dilution of 1:500 (Research Diagnostics, Inc., Flanders, NJ). Secondary antibodies were Alexa Fluor 488-conjugated goat anti-rabbit IgG (Molecular Probes, Inc., Eugene, OR) and tetrarhodamine isothiocyanate

(TRITC) -conjugated rabbit anti-mouse IgG (Sigma-Aldrich); both secondary antibodies were used at dilution of 1:500.

Immunofluorescence

Mouse embryos or isolated hearts were fixed for 1 hr at 4°C in 4% formaldehyde plus phosphate buffered saline (PBS). The fixed samples were washed with cold PBS, and then equilibrated in 20% sucrose plus PBS at 4°C. Samples were embedded in O.C.T. compound (Sakura Finetek U.S.A., Inc., Torrance, CA) and frozen on dry ice. Embryos were oriented to yield sagittal sections, and frozen sections 15 μm thick were cut on a Hacker cryostat (Hacker Instruments, Winnsboro, SC).

Sections were permeabilized in 0.4% Triton X-100 for 30 min and blocked in 10% normal goat serum for 1 hr. After blocking, sections were incubated with a mixture of rabbit polyclonal antibody against N-RAP and mouse monoclonal antibody against either α-actinin or N-cadherin overnight in the presence of 10% goat serum. Negative controls were obtained using serial sections of the same specimens in which nonimmune rabbit serum was substituted for the anti–N-RAP serum. Secondary labeling was performed with Alexa Fluor 488-conjugated goat anti-rabbit antibody and subsequently with TRITC-conjugated rabbit anti-mouse secondary antibodies for 2 hr each in the presence of 10% goat serum. All incubations were at room temperature in PBS, pH 7.4, which was also used to wash the sections in between incubations. Nuclei were visualized with 4′,6-diamidino-2-phenylindole-dihydrochloride (DAPI). Stained sections were mounted in Vectashield mounting medium (Vector Laboratories, Burlingame, CA).

Microscopy and Image Processing

Stained sections were observed with a Zeiss Axiovert 135 microscope equipped for incident-light fluorescence as well as phase contrast and brightfield microscopy. Appropriate excitation filters for Alexa fluor 488, TRITC, and DAPI were mounted in a computer controlled filter wheel (Ludl

Electronic Products, Ltd., Hawthorne, NY), and a single broadband emission filter was used for all fluorophores. Oil immersion ×63 and ×100 objectives with numerical apertures of 1.25 and 1.30, respectively, were used. Low magnification views were obtained using a dry ×10 objective with numerical aperture of 0.3. Fluorescent images were collected using a Photometrics CoolSnap fx CCD camera (Roper Scientific, Inc., Tucson, AZ) interfaced with a Power Macintosh computer.

Fluorescent images were processed on a Power Macintosh computer using IPLab software (Scanalytics, Inc., Fairfax, VA). Background levels of N-RAP staining were estimated from the intensity histogram of photomicrographs of similar regions from serial sections of the same specimens in which nonimmune rabbit serum was substituted for the anti–N-RAP serum; the background level was then subtracted using a level adjustment that remapped the dynamic range so that background levels became black and the brightest staining in the N-RAP stained sections were maximized. In images captured using the ×100 and ×63 objectives, out of focus fluorescence was removed by digital deconvolution using MicroTome software (VayTek, Inc., Fairfield, IA). In each case, identical level adjustments and deconvolution settings were used for the nonimmune control and the N-RAP stained serial sections from the same specimen.

Triple-staining data are presented with rhodamine, Alexa Fluor 488 and DAPI fluorescence in the red, green, and blue channels, respectively. For presentation of double-staining, rhodamine fluorescence is presented as magenta (equal parts red and blue) to facilitate access by color-blind individuals. (See http://jfly.nibb.ac.jp/html/color_blind for reference.) With this presentation method, colocalization appears white in composite images due to the combination of magenta and green.

REFERENCES

Arber S, Halder G, Caroni P. 1994. Muscle LIM protein, a novel essential regulator of myogenesis, promotes myogenic differentiation. Cell 79:221–231.

Arber S, Hunter JJ, Ross J Jr, Hongo M, Sansig G, Borg J, Perriard JC, Chien KR, Caroni P. 1997. MLP-deficient mice exhibit a disruption of cardiac cytoarchitectural organization, dilated cardiomyopathy, and heart failure. Cell 88:393–403.

Carroll SL, Horowits R. 2000. Myofibrillogenesis and formation of cell contacts mediate the localization of N-RAP in cultured chick cardiomyocytes. Cell Motil Cytoskeleton 47:63–76.

Carroll SL, Herrera AH, Horowits R. 2001. Targeting and functional role of N-RAP, a nebulin-related LIM protein, during myofibril assembly in cultured chick cardiomyocytes. J Cell Sci 114:4229–4238.

Carroll S, Lu S, Herrera AH, Horowits R. 2004. N-RAP scaffolds I-Z-I assembly during myofibrillogenesis in cultured chick cardiomyocytes. J Cell Sci 117:105–114.

Chomczynski P, Sacchi N. 1987. Single-step method of RNA isolation by acid guanidinium thiocyanate-phenol-chloroform extraction. Anal Biochem 162:156–159.

Dabiri GA, Turnacioglu KK, Sanger JM, Sanger JW. 1997. Myofibrillogenesis visualized in living embryonic cardiomyocytes. Proc Natl Acad Sci U S A 94:9493–9498.

Dlugosz AA, Antin PB, Nachmias VT, Holtzer H. 1984. The relationship between stress fiber-like structures and nascent myofibrils in cultured cardiac myocytes. J Cell Biol 99:2268–2278.

Du A, Sanger JM, Linask KK, Sanger JW. 2003. Myofibrillogenesis in the first cardiomyocytes formed from isolated quail precardiac mesoderm. Dev Biol 257:382–394.

Ehler E, Rothen BM, Hämmerle SP, Komiyama M, Perriard J-C. 1999. Myofibrillogenesis in the developing chicken heart: assembly of the z-disk, m-line and thick filaments. J Cell Sci 112:1529–1539.

Ehler E, Horowits R, Zuppinger C, Price RL, Perriard E, Leu M, Caroni P, Sussman A, Eppenberger HM, Perriard JC. 2001. Alterations at the intercalated disk associated with the absence of muscle LIM protein. J Cell Biol 153:763–772.

Forbes MS, Sperelakis N. 1985. Intercalated discs of mammalian heart: a review of structure and function. Tissue Cell 17:605–648.

Gehmlich K, Geier C, Osterziel KJ, Van Der Ven PF, Furst DO. 2004. Decreased interactions of mutant muscle LIM protein (MLP) with N-RAP and alpha-actinin and their implication for hypertrophic cardiomyopathy. Cell Tissue Res 317:129–136.

Geier C, Perrot A, Ozcelik C, Binner P, Counsell D, Hoffmann K, Pilz B, Martiniak Y, Gehmlich K, van der Ven PF, Furst DO, Vornwald A, von Hodenberg E, Nurnberg P, Scheffold T, Dietz R, Osterziel KJ. 2003. Mutations in the human muscle LIM protein gene in families with hypertrophic cardiomyopathy. Circulation 107:1390–1395.

Geiger B, Ayalon O. 1992. Cadherins. Annu Rev Cell Biol 8:307–332.

Handel SE, Greaser ML, Schultz E, Wang SM, Bulinski JC, Lin JJ, Lessard JL. 1991. Chicken cardiac myofibrillogenesis studied with antibodies specific for titin and the muscle and nonmuscle isoforms of actin and tropomyosin. Cell Tissue Res 263:419–430.

Herrera AH, Elzey B, Law DJ, Horowits R. 2000. Terminal regions of mouse nebulin: sequence analysis and complementary localization with N-RAP. Cell Motil Cytoskeleton 45:211–222.

Hertig CM, Eppenberger-Eberhardt M, Koch S, Eppenberger HM. 1996. N-cadherin in adult rat cardiomyocytes in culture. I. Functional role of N-cadherin and impairment of cell-cell contact by a truncated N- cadherin mutant. J Cell Sci 109:1–10.

Holtzer H, Hijikata T, Lin ZX, Zhang ZQ, Holtzer S, Protasi F, Franzini-Armstrong C, Sweeney HL. 1997. Independent assembly of 1.6 microns long bipolar MHC filaments and I-Z-I bodies. Cell Struct Funct 22:83–93.

Imanaka-Yoshida K, Knudsen KA, Linask KK. 1998. N-cadherin is required for the differentiation and initial myofibrillogenesis of chick cardiomyocytes. Cell Motil Cytoskeleton 39:52–62.

Kemler R. 1993. From cadherins to catenins: cytoplasmic protein interactions and regulation of cell adhesion. Trends Genet 9:317–321.

Knoll R, Hoshijima M, Hoffman HM, Person V, Lorenzen-Schmidt I, Bang ML, Hayashi T, Shiga N, Yasukawa H, Schaper W, McKenna W, Yokoyama M, Schork NJ, Omens JH, McCulloch AD, Kimura A, Gregorio CC, Poller W, Schaper J, Schultheiss HP, Chien KR. 2002. The cardiac mechanical stretch sensor machinery involves a Z disc complex that is defective in a subset of human dilated cardiomyopathy. Cell 111:943–955.

Kong Y, Flick MJ, Kudla AJ, Konieczny SF. 1997. Muscle LIM protein promotes myogenesis by enhancing the activity of MyoD. Mol Cell Biol 17:4750–4760.

Kruger M, Wright J, Wang K. 1991. Nebulin as a length regulator of thin filaments of vertebrate skeletal muscles: correlation of thin filament length, nebulin size, and epitope profile. J Cell Biol 115:97–107.

Labeit S, Kolmerer B. 1995. The complete primary structure of human nebulin and its correlation to muscle structure. J Mol Biol 248:308–315.

Labeit S, Gibson T, Lakey A, Leonard K, Zeviani M, Knight P, Wardale J, Trinick J. 1991. Evidence that nebulin is a protein-ruler in muscle thin filaments. FEBS Lett 282:313–316.

Lin ZX, Holtzer S, Schultheiss T, Murray J, Masaki T, Fischman DA, Holtzer H. 1989. Polygons and adhesion plaques and the disassembly and assembly of myofibrils in cardiac myocytes. J Cell Biol 108:2355–2367.

Lu S, Carroll SL, Herrera AH, Ozanne B, Horowits R. 2003. New N-RAP-binding partners α-actinin, filamin and Krp1 detected by yeast two-hybrid screening: implications for myofibril assembly. J Cell Sci 116:2169–2178.

Luo G, Zhang JQ, Nguyen TP, Herrera AH, Paterson B, Horowits R. 1997. Complete cDNA sequence and tissue localization of N-RAP, a novel nebulin-related protein of striated muscle. Cell Motil Cytoskeleton 38:75–90.

Luo G, Herrera AH, Horowits R. 1999. Molecular interactions of N-RAP, a nebulin-related protein of striated muscle myotendon junctions and intercalated disks. Biochemistry 38:6135–6143.

Mills M, Yang N, Weinberger R, Vander Woude DL, Beggs AH, Easteal S, North K. 2001. Differential expression of the actin-binding proteins, alpha-actinin-2 and -3, in different species: implications for the evolution of functional redundancy. Hum Mol Genet 10:1335–1346.

Mohiddin SA, Lu S, Cardoso J-P, Carroll SL, Jha S, Horowits R, Fananapazir L. 2003. Genomic organization, alternative splicing, and expression of human and mouse N-RAP, a nebulin-related LIM protein of striated muscle. Cell Motil Cytoskeleton 55:200–212.

Radice GL, Rayburn H, Matsunami H, Knudsen KA, Takeichi M, Hynes RO. 1997. Developmental defects in mouse embryos lacking N-cadherin. Dev Biol 181:64–78.

Rhee D, Sanger JM, Sanger JW. 1994. The premyofibril: evidence for its role in myofibrillogenesis. Cell Motil Cytoskeleton 28:1–24.

Rudy DE, Yatskievych TA, Antin PB, Gregorio CC. 2001. Assembly of thick, thin, and titin filaments in chick precardiac explants. Dev Dyn 221:61–71.

Schultheiss T, Lin ZX, Lu MH, Murray J, Fischman DA, Weber K, Masaki T, Imamura M, Holtzer H. 1990. Differential distribution of subsets of myofibrillar proteins in cardiac nonstriated and striated myofibrils. J Cell Biol 110:1159–1172.

Severs NJ. 1995. Cardiac muscle cell interaction: from microanatomy to the molecular make-up of the gap junction. Histol Histopathol 10:481–501.

Soler AP, Knudsen KA. 1994. N-cadherin involvement in cardiac myocyte interaction and myofibrillogenesis. Dev Biol 162:9–17.

Sussman MA, Welch S, Cambon N, Klevitsky R, Hewett TE, Price R, Witt SA, Kimball TR. 1998. Myofibril degeneration caused by tropomodulin overexpression leads to dilated cardiomyopathy in juvenile mice. J Clin Invest 101:51–61.

Takeichi M. 1990. Cadherins: a molecular family important in selective cell–cell adhesion. Annu Rev Biochem 59:237–252.

Wang SM, Greaser ML, Schultz E, Bulinski JC, Lin JJ, Lessard JL. 1988. Studies on cardiac myofibrillogenesis with antibodies to titin, actin, tropomyosin, and myosin. J Cell Biol 107:1075–1083.

Wang K, Knipfer M, Huang QQ, van Heerden A, Hsu LC, Gutierrez G, Quian XL, Stedman H. 1996. Human skeletal muscle nebulin sequence encodes a blueprint for thin filament architecture: sequence motifs and affinity profiles of tandem repeats and terminal SH3. J Biol Chem 271:4304–4314.

Zhang JQ, Elzey B, Williams G, Lu S, Law DJ, Horowits R. 2001. Ultrastructural and biochemical localization of N-RAP at the interface between myofibrils and intercalated disks in the mouse heart. Biochemistry 40:14898–14906.